NUCLEAR SCIENCE AND ENGINEERING: 83, 50-62 (1983)

Critical Experiments on Gadolinium Poisoned Cluster-Type Fuel Assemblies in Heavy Water Lattices

Toshio Wakabayashi and Isao Minatsuki*

Oarai Engineering Center, Power Reactor and Nuclear Fuel Development Corporation
4002 Oarai-machi, Ibaraki-ken, Japan

Received April 6, 1982
Accepted July 7, 1982

The physical behavior of burnable poison fuel pins, containing 0.1, 0.5, and 1.0 wt% Gd_2O_3 in 1.5 wt% UO_2 pellets, has been studied through the measurements of reactivity change, coolant void reactivity, local power distribution, and thermal neutron flux distribution including fine structure, using a heavy-water-moderated, cluster-type fuel lattice.

A new technique for utilizing a burnable poison has been developed using a gadolinium absorber rod inserted into the center of the cluster-type fuel assembly. Its physical behavior has been studied through the measurements of accompanying reactivity change, coolant void reactivity, local power distribution, and thermal neutron flux distribution.

When the Gd_2O_3 content of the fuel pellets is more than 0.5 wt%, the reactivity effect is reduced largely due to the saturation of the thermal neutron self-shielding effect in the poisoned fuel pin.

A gadolinium absorber rod inserted in the center of the fuel assembly, although it causes a small increase in local power peaking, is effective in the control of the initial excess reactivity and favorably affects the coolant void reactivity.

An accurate calculation by the WIMS-D code requires division of the fuel pellet region into more than five mesh intervals owing to the enhancement of the thermal neutron self-shielding effect due to absorption by the gadolinium in the poisoned fuel pins.

I. INTRODUCTION

A burnable poison mixed in the fuel pellets of light water power reactors[1,2] has been employed to control the initial excess reactivity and the power distributions. This suggests that the use of burnable poison in a heavy-water-moderated, light-water-cooled thermal reactor (HWR) (Refs. 3 and 4) might also be effective in reducing the initial excess reactivity and improving the power distribution, resulting in an extension of the power cycle length.

Since a heavy-water-moderated, cluster-type fuel lattice is highly heterogeneous, the neutron behavior in the lattice is more complicated[5-7] than that in the regular H_2O lattice of single fuel pins. The thermal neutron flux distribution is particularly highly depressed in the center of a fuel cluster. It is considered

*Present address: FBR Engineering Company, Ltd., Shin-Aoyama Bldg Nishikan 12F, 1-1-1 Minamiaoyama, Minato-ku, Tokyo, Japan.

[1]K. P. TERMAAT, *Nucl. Technol.*, 38, 367 (1978).
[2]T. HAGA, S. HANAZAWA, and T. KIMURA, *Nucl. Sci. Eng.*, 69, 231 (1979).
[3]S. SHIMA and S. SAWAI, "The Fugen Project," *Proc. 13th Ann. Int. Conf.*, Toronto, June 17-20, 1973, CNA'73-204, Canadian Nuclear Association (1973).
[4]S. SAWAI, M. AKEBI, T. HAGA, and K. KONTANI, *Nucl. Eng. Int.*, 24, 33 (1979).
[5]Y. HACHIYA and H. HATAKENAKA, *J. Nucl. Sci. Technol.*, 9(II), 629 (1972).
[6]Y. HACHIYA, N. FUKUMURA, A. NISHI, K. IIJIMA, and H. SAKATA, *J. Nucl. Sci. Technol.*, 13(II), 618 (1976).
[7]T. WAKABAYASHI and Y. HACHIYA, *Nucl. Sci. Eng.*, 63, 292 (1977).

0029-5639/83/0001-0050$03.00/0

that the physical behavior of the burnable poison in the cluster-type fuel lattice is largely affected by such changes as the content of poison in fuel pellets, the number and location of poisoned fuel pins in a fuel cluster, and the coolant voiding. Accordingly, many experiments are required for clarification of the physical behavior and for the evaluation and the improvement of calculational accuracy concerning burnable poisons in the cluster-type fuel lattice. There have been, however, few experimental studies of burnable poisons.[8]

In addition to the use of a burnable poison in fuel pellets, consideration has been given to a burnable poison as an absorber rod inserted in the center of the cluster-type fuel assembly to effectively control initial excess reactivity and for improvement of the power distribution and the coolant void reactivity.[9]

The main objective of the present experiment is to make the changes in nuclear characteristics clear for the purpose of confirming the advantage of employing gadolinium poisoned fuel pins and a gadolinium absorber rod in the HWR from the viewpoint of fuel design. Therefore, measurements were made on the reactivity change, coolant void reactivity, local power distribution, and thermal neutron flux distribution, including fine structure, under various parameters, particularly the gadolinium content and the coolant voiding, using the deuterium critical assembly (DCA). Experimental results are compared with calculations by the use of the WIMS-D code[10] and the CITATION code.[11]

II. EXPERIMENTAL METHOD AND PROCEDURE

A test fuel cluster used for the present experiments consists of 54 fuel pins composed of UO_2 enriched to 1.5 wt% in ^{235}U as shown in Fig. 1. The fuel pins in the cluster were arranged in three concentric layers; outward from the center there are 12 pins in the first layer, 18 in the second, and 24 in the third.

As shown in Fig. 2, the test fuel cluster was placed at the center of the DCA and was surrounded by 136 driver fuel clusters of 28 pins each. The 28-pin driver cluster fueled with 1.2 wt% ^{235}U-enriched UO_2, as shown in Fig. 3, was housed in an air-filled pressure tube and was arranged in a square lattice of 20.0-cm pitch.

The heavy water used as moderator was of 99.4 mol% purity. Throughout the experiment all the components were maintained at the ambient temperature of 22°C.

To investigate the effect of burnable poison in fuel pellets, a few fuel pins of the 54-pin cluster were replaced with 1.5 wt% enriched UO_2 pins containing 0.1, 0.5, or 1.0 wt% Gd_2O_3. The specifications of unpoisoned and poisoned fuel pins are listed in Table I.

An absorber rod to be inserted in the center of the 54-pin cluster was made of gadolinium sulfate powder contained in an aluminum tube having the same dimensions as those of the unpoisoned fuel pins. The powder was vibration-compacted to 74.8% of its theoretical density.

II.A. Reactivity Change

Reactivity changes determined from change in critical D_2O height, resulting from substitutions of poisoned fuel pins for unpoisoned ones were measured as functions of

1. poison content (0.1, 0.5, and 1.0 wt% Gd_2O_3)
2. number of poisoned fuel pins (1, 2, and 12)
3. configuration of the poisoned fuel pins within a cluster (first, second, and third layer)
4. coolant voiding (0 and 100% void fraction).

Reactivity changes produced by the insertion of the gadolinium absorber rod were also measured as function of coolant voiding. The arrangements of the burnable poison in the 54-pin cluster are shown in Fig. 4.

Reactivities were obtained by integrating the D_2O level coefficient of reactivity over the change in critical D_2O height. This coefficient in cents per centimetre is defined as follows by the one-group diffusion theory:

$$\frac{\partial \rho}{\partial H} = \frac{1}{\beta_{eff}} \cdot \frac{2\pi^2 M^2}{k_\infty} \cdot \frac{1}{(H+\delta)^3} = \frac{\alpha}{(H+\delta)^3} \cdot \quad (1)$$

where

β_{eff} = effective delayed neutron fraction

M^2 = migration area

k_∞ = infinite neutron multiplication factor

$\alpha = 2\pi^2 M^2/\beta_{eff} k_\infty$ (cent·cm^2)

H = D_2O height (cm)

δ = effective axial extrapolation distance (cm).

---

[8] I. MINATSUKI and T. WAKABAYASHI, *Trans. Am. Nucl. Soc.*, 32, 779 (1979).

[9] T. WAKABAYASHI and I. MINATSUKI, "Fuel Cluster Design for Improvement of Coolant Void Reactivity and Local Power Peaking," *Proc. 19th Ann. Int. Conf.*, Toronto, June 10-13, 1979, Canadian Nuclear Association (1979).

[10] J. R. ASKEW, F. J. DAYERS, and F. B. KEMSHELL, *J. Brit. Nucl. Soc.*, 5, 564 (1966).

[11] T. B. FOWLER, D. R. VONDY, and G. W. CUNNINGHAM, "Nuclear Reactor Core Analysis Code: CITATION," ORNL-TM-2496 Rev. 2, Oak Ridge National Laboratory (1971).

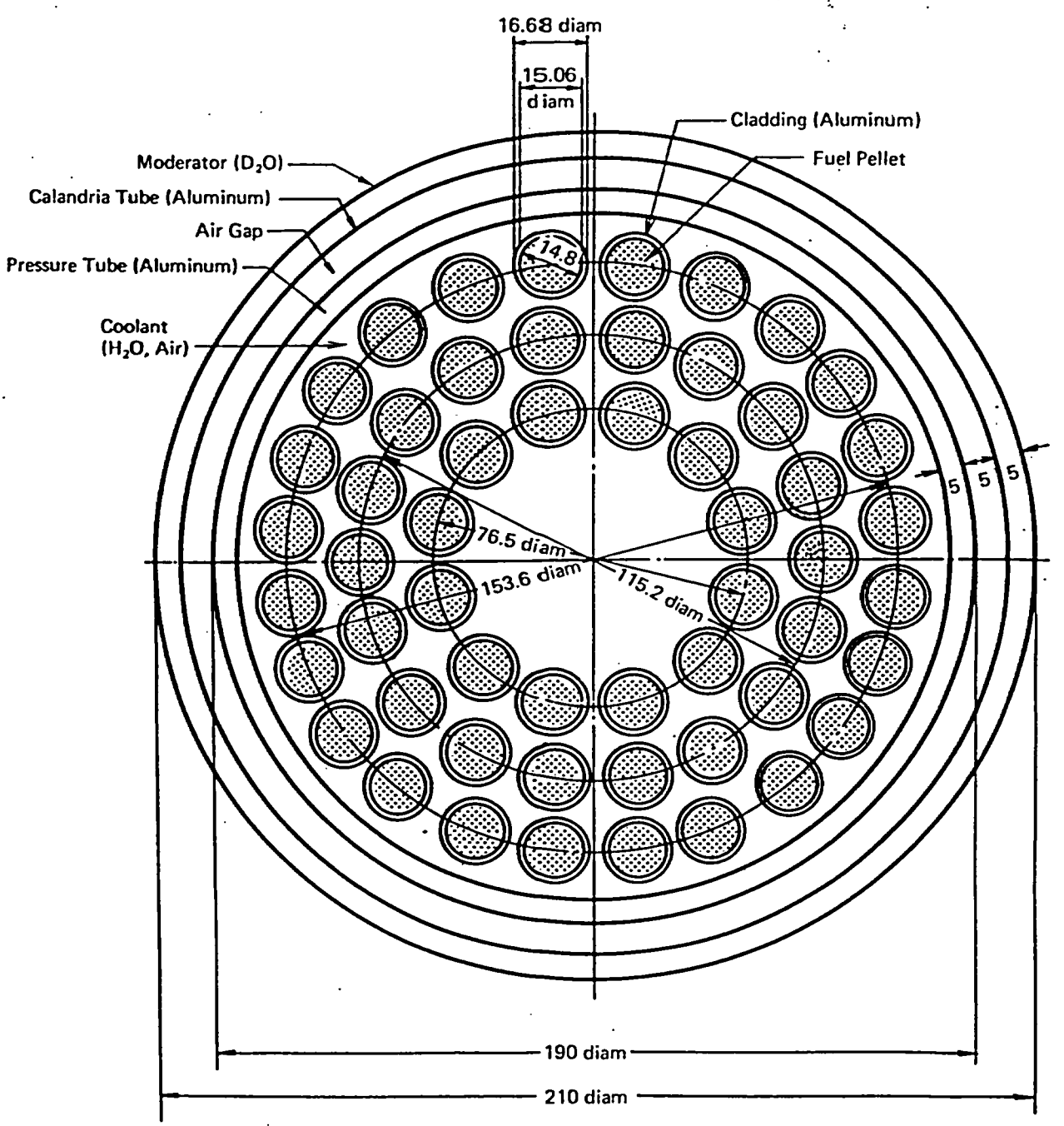

Fig. 1. Cross-sectional view of a 54-pin test fuel cluster. (Dimensions are in millimetres.)

The axial distribution of copper activation measured at the center of the 54-pin cluster was fitted to a cosine function to determine the effective axial extrapolation distance. The value of δ was 14.4 ± 1.5 cm.

The D_2O level coefficients of reactivity were obtained by the positive period method at various critical D_2O heights.[12] The periods were measured after raising the D_2O level by 2 to 5 mm from criticality. Values of α were obtained from the measured reactivity coefficients and critical D_2O heights using Eq. (1). The variation in α value with the critical heights was within the experimental

[12]T. OTSUKA, N. FUKUMURA, and Y. HACHIYA, *Nucl. Sci. Eng.*, **74**, 95 (1980).

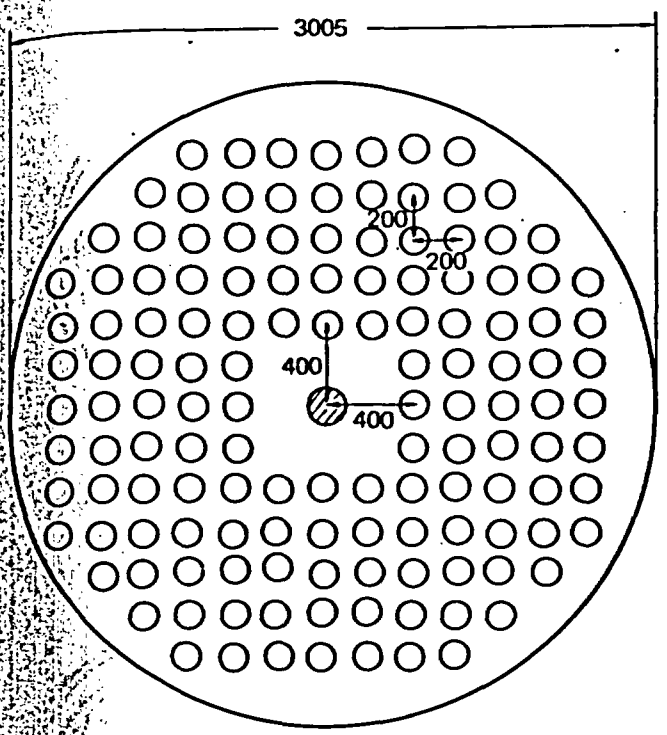

Fig. 2. Configuration of fuel clusters in DCA. (Dimensions are in millimetres.)

uncertainty (±4%). Consequently, the α was assumed constant, and all the values of α were averaged.

Reactivities, in cents, corresponding to the change in critical D_2O height from h_1 to h_2 were evaluated by

$$\rho = \int_{h_1}^{h_2} \left(\frac{\partial \rho}{\partial H}\right) dH = \left(\frac{\alpha}{2}\right)\left[\frac{1}{(h_1+\delta)^2} - \frac{1}{(h_2+\delta)^2}\right] . \quad (2)$$

Measurements of the D_2O height were made to an accuracy of 0.2 mm (±0.02%) with the use of a survo-manometer (level meter) in a communicating tube attached to the DCA tank. The coolant height for the reference lattice was kept to within 1 mm of the critical D_2O height. Therefore, the error in the reactivity obtained by Eq. (2) was estimated as ±4%.

II.B. Coolant Void Reactivity

The coolant void reactivity was measured first in the unpoisoned 54-pin cluster and then in the 54-pin cluster with poisoned fuel pins or with the gadolinium absorber rod. Reactivities due to the loss of coolant in the fuel clusters were determined from calibrated changes in the D_2O moderator level. This is, the reactivity change corresponding to a change in the D_2O height from h_1 (at 0% void fraction) to h_2 (at 100% void fraction) was obtained by Eq. (2).

TABLE I

Specification of Fuel

Fuel Type	Normal Fuel Pin	Nominal 0.1 wt% Gd_2O_3 Poisoned Fuel Pin	Nominal 0.5 wt% Gd_2O_3 Poisoned Fuel Pin	Nominal 1.0 wt% Gd_2O_3 Poisoned Fuel Pin
Fuel pellet				
Density (g/cm³)	10.38	10.30	10.30	10.30
Diameter (mm)	14.77	14.78	14.78	14.78
^{235}U content of UO_2 (wt%)	1.5	1.5	1.5	1.5
Gd_2O_3 content (wt%)	---	0.10	0.496	0.993
Composition of pellet (wt%)				
^{235}U	1.317	1.328	1.323	1.316
^{238}U	86.563	86.384	86.042	85.612
^{16}O	12.120	12.201	12.205	12.210
^{155}Gd	---	0.01278	0.06335	0.12690
^{157}Gd	---	0.01360	0.06748	0.13509
Other gadolinium	---	0.06	0.30	0.60
Fuel pin				
Cladding material	Aluminum	Aluminum		
Cladding i.d. (mm)	15.03	14.98		
Cladding o.d. (mm)	16.73	16.69		
Gap material	Air	Air		

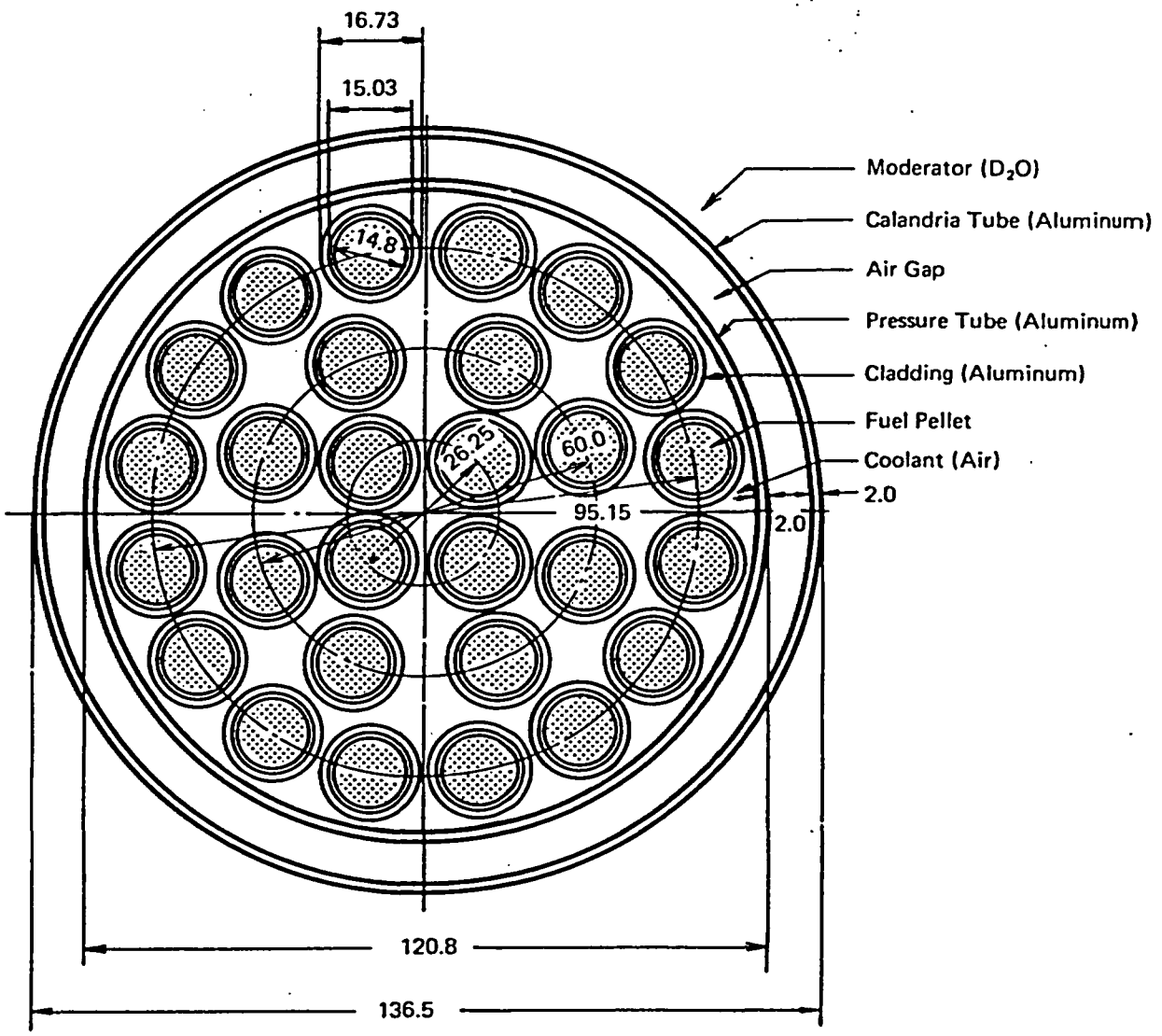

Fig. 3. Cross-sectional view of a 28-pin driver fuel cluster. (Dimensions are in millimetres.)

II.C. Local Power Distribution

Local power distributions in the 54-pin cluster and the 54-pin cluster with 12 poisoned fuel pins or with the gadolinium absorber rod were measured by means of the foil activation method using 0.1-mm-thick, 14.8-mm-diam 93% ^{235}U-enriched U(10%)-Al alloy foils. Natural uranium metal foils were also irradiated in the same fuel pins. The foils were used to determine the ^{238}U-to-^{235}U fission reaction rate ratio.

The uranium foils were covered with 0.02-mm-thick aluminum as a cassette to prevent contamination by UO_2 powder and fission products.[5,6] The foil cassettes were loaded together with fuel pellets into the aluminum tubes, and set at positions F-1, F-2, F-3-1, and F-3-2 for the 54-pin clusters with or without the gadolinium rod, and F-1, F-2-1, F-2-2, F-2-3, F-3-1, and F-3-2 for the 54-pin cluster with 12 poisoned fuel pins as shown in Fig. 4. The foils were irradiated for 30 min at 500 W (~10^9 n/cm^2·s). After irradiation, gamma rays from fission products in the foils were measured by a 2-in.-diam X 2-in.-thick NaI(Tl) detector.

II.D. Thermal Neutron Flux Distribution

Thermal neutron flux distributions in the 54-pin cluster and the 54-pin cluster with 12 poisoned fuel pins or the gadolinium absorber rod were measured in the fuel pins, on the surfaces of the pressure and the calandria tubes, and in the D_2O moderator around them, by the use of 0.1-mm-thick dysprosium-aluminum alloy foils (dysprosium content = 4.0 wt%). The 14.8-mm-diam dysprosium-aluminum alloy foils were packed in the same fuel pins and in the

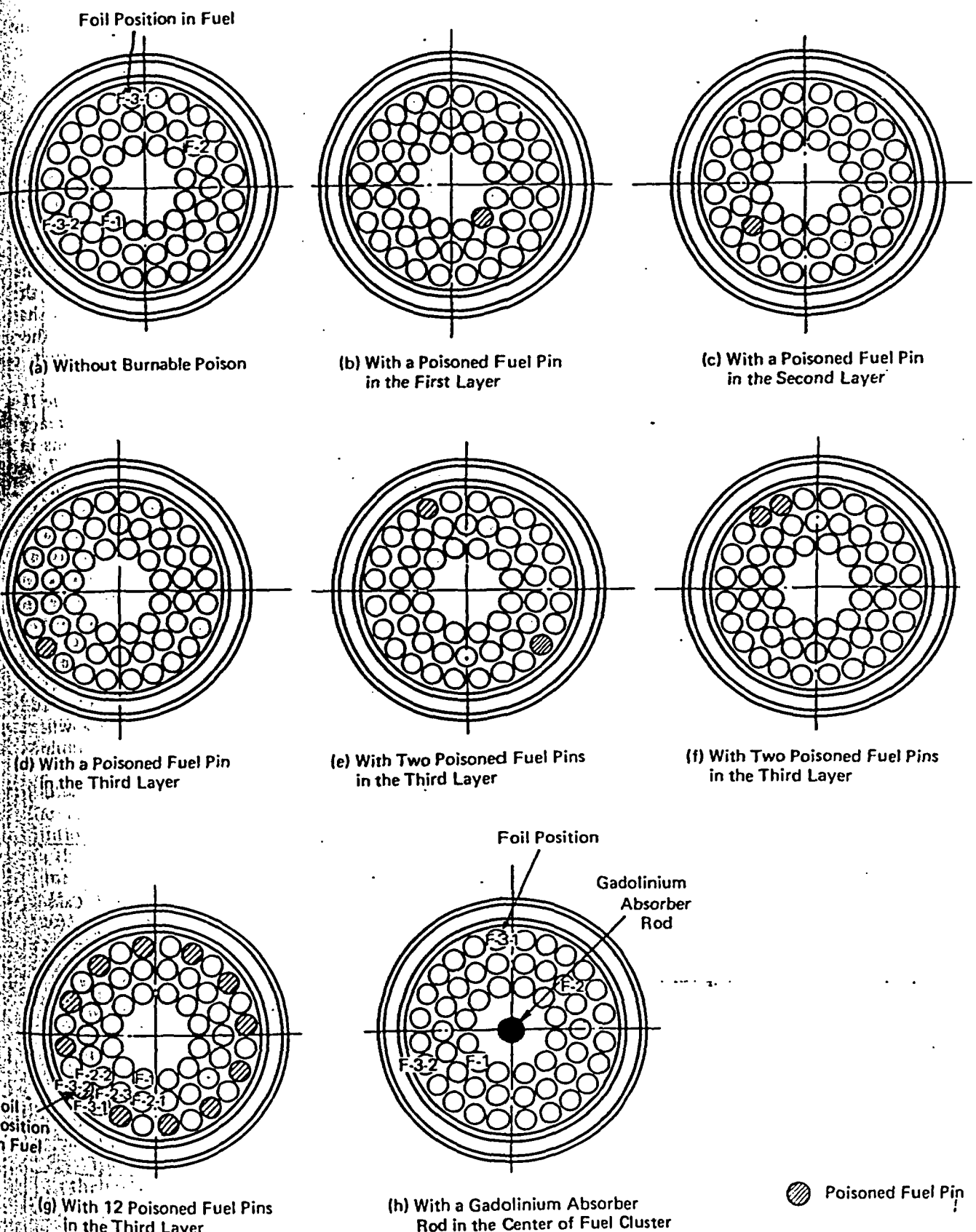

Fig. 4. Burnable poison and foil arrangement in a 54-pin cluster.

same way as were uranium foils. To measure the thermal neutron flux on the surfaces of the pressure and the calandria tubes, 7-mm-diam dysprosium foils were set at two symmetrical positions around each surface. The thermal neutron flux distribution in the D_2O-moderator region was measured using the same 7-mm-diam foils. In this measurement, the foils were arranged along a radius with a 10-mm spacing supported by a 0.5-mm-thick aluminum holder.[7]

The dysprosium foils were irradiated at the same elevation, 60 cm from the lower grid plate. After irradiation, beta rays from ^{165}Dy (half-life = 139.9 min) were counted by a 2-in.-diam × $\frac{1}{8}$-in.-thick $CaF_2(Eu)$ scintillator. Measured activities of the dysprosium foils were corrected for background and dead time, the decay time, and the counting efficiency characteristic of the various foil shapes and weights.

II.E. Fine Structure of Thermal Neutron Flux Distribution

To study the self-shielding effect of gadolinium in the fuel pellet, the fine structures of the thermal neutron flux distribution were measured by activating dysprosium foils inserted between fuel pellets containing 0.1, 0.5, or 1.0 wt% Gd_2O_3. These fuel pins were located in the center of the D_2O-moderator region to reduce the interference of the thermal neutron flux depression in the fuel cluster. After irradiation, the foils were divided into eight or nine concentric sections; each section was then counted for a time, depending on its activity and counting efficiency.

III. RESULTS AND DISCUSSION

III.A. Reactivity Change

The changes in reactivity due to substitution of poisoned fuel pins for unpoisoned ones are shown in Table II. The experimental error in these results was estimated to be ±4%. The upper three entries clearly show the dependence of the reactivity change on the Gd_2O_3 content of the fuel pin. As shown in Fig. 5, the reactivity does not decrease so sharply above 0.5 wt% Gd_2O_3 because of the onset of thermal neutron self-shielding by gadolinium at that concentration.

The data in Cases 1, 7, 8, and 9 of Table II and in Fig. 6 show the dependence of the reactivity change on the number of poisoned fuel pins in the fuel cluster. The reactivity change in Case 7, which is due to the substitution of two poisoned fuel pins sufficiently spaced, is in good agreement with twice the reactivity change in Case 1 for a single poisoned fuel pin. On the other hand, the reactivity change in Case 8 due to two poisoned fuel pins close to each other, is smaller by ~15% than twice the reactivity in Case 1. Furthermore, the reactivity change shown in Case 9 with 12 poisoned fuel pins inserted in alternate positions is smaller by ~40% than 12 times the reactivity in the first case. These behaviors of reactivity changes show that two or more poisoned fuel pins largely interfere with each

TABLE II

Comparison of Reactivity Change Between Experiment and Calculation

Case Number	Fuel and Absorber Type	Absorber			Coolant Void Fraction (%)	Experiment (cents)	Calculation (cents)
		Arrangement in Cluster	Number of Pins	Gd_2O_3 Content (wt%)			
1	54-pin cluster with poisoned fuel pin	Third layer	1	1.0	0	−53.8	−55.5
2		Third layer	1	0.5	0	−51.6	−52.1
3		Third layer	1	0.1	0	−36.1	−37.7
4		Third layer	1	1.0	100	−69.0	−74.0
5		Second layer	1	1.0	0	−40.6	−37.6
6		First layer	1	1.0	0	−38.4	−35.0
7		Third layer	2	1.0	0	−107.2	−103.9
8		Third layer	2[a]	1.0	0	−90.4	−89.1
9		Third layer	12	1.0	0	−356.4	−388.5
10		Third layer	12	1.0	100	−430.8	−467.9
11	54-pin cluster with gadolinium absorber rod	Center of cluster	1	---	0	−47.1	−43.6
12			1	---	100	−55.5	−55.4

[a]The pins were adjacent in this case.

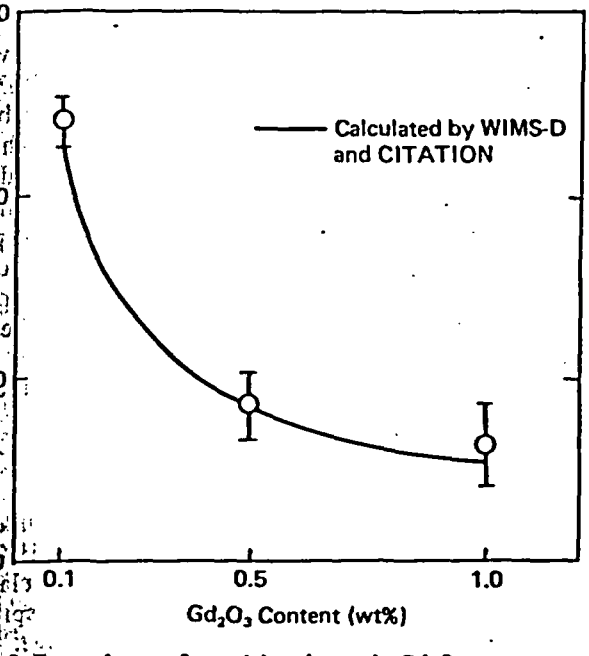

Fig. 5. Dependence of reactivity change in Gd_2O_3 content.

other, particularly where their spacing is small. The interference suggests that the gadolinium depresses the thermal neutron flux in the vicinity of a poisoned fuel pin.

The data in Cases 1, 5, and 6 in Table II show the dependence of the reactivity change on the position of a poisoned fuel pin. As shown in Fig. 7, the reactivity change decreases as the position of the gadolinium approaches the center of the fuel cluster due to a depression of the thermal neutron flux distribution in the center of the fuel cluster.

The reactivity change in Case 4, due to fuel substitution in the air-filled cluster, is larger than that in the H_2O-filled cluster of Case 1; furthermore, the same tendency is shown in Cases 9 and 10 of Table II. This behavior in reactivity change can be attributed to the fact that neutron absorption in a poisoned fuel pin increases due to the smaller depression of the neutron flux in the air-filled cluster, because the thermal neutron diffusion depression effect enhanced by the H_2O coolant is not present in this air-filled cluster.

Reactivity changes introduced by the insertion of the gadolinium absorber rod in the 54-pin cluster are shown in Cases 11 and 12 of Table II. It is clear that the insertion of the rod in the center of the fuel cluster is effective for the control of excess reactivity. Table II also shows the results calculated by using the WIMS-D and the CITATION codes.

The WIMS-D code is a general lattice cell program that uses transport theory to calculate flux as a function of energy and position in a cell. The basic cross-section library is in 69 groups with 14 fast,

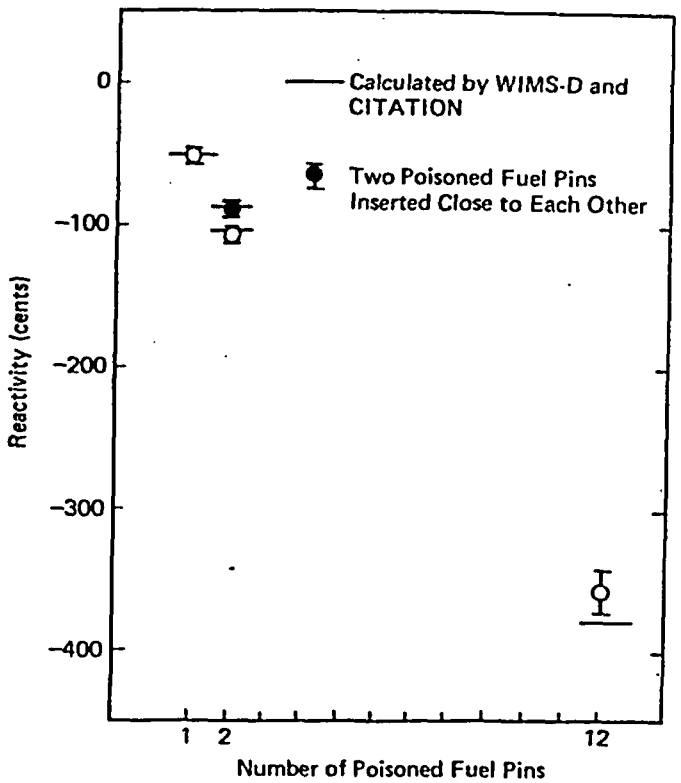

Fig. 6. Dependence of reactivity change on the number of poisoned fuel pins (1.0 wt% Gd_2O_3).

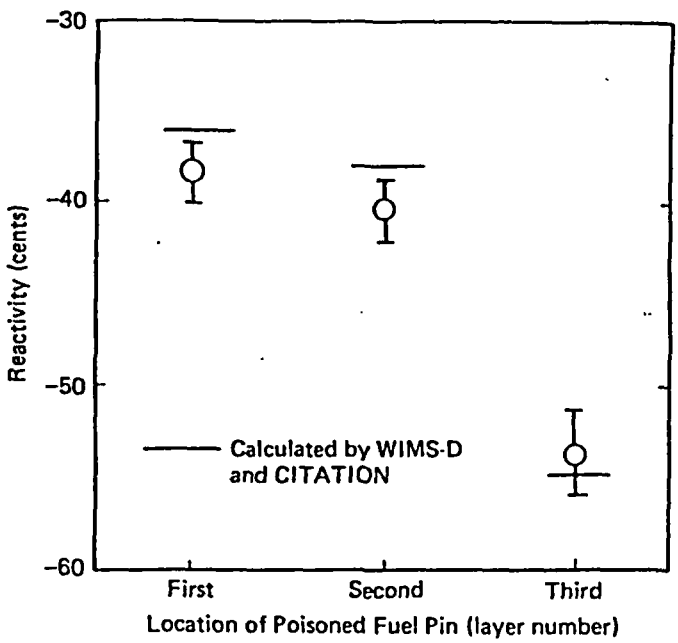

Fig. 7. Dependence of reactivity change on the position of the poisoned fuel pin in the fuel cluster (1.0 wt% Gd_2O_3).

13 resonance, and 42 thermal groups. The transport equation is solved by a collision probability method using up to 69 neutron energy groups. Besides producing few group cell-averaged constants, point-by-point reaction rates over the entire energy range are calculated for detectors such as dysprosium, manganese, and copper.

In the present cell calculation, cross sections of ^{155}Gd and ^{157}Gd prepared from the ENDF/B-III library[13] were added to the original WIMS-D library, and the 69 energy groups were condensed into 15. Five mesh intervals in fuel pellets were used according to the results of the analysis of the fine structure of the thermal neutron flux distribution in Sec.III.E.

Reactivity changes for the whole core were calculated in a diffusion approximation of four groups using cell-averaged constants produced by WIMS-D. The two-dimensional X-Y model of the DCA core was employed for this calculation using CITATION. The calculational results are in good agreement with the experimental ones within 9%.

III.B. Coolant Void Reactivity

Experimental fractional reductions in coolant void reactivity are shown in Table III with the results also calculated by WIMS-D and CITATION. The use of poisoned fuel pins and the insertion of the gadolinium absorber rod in the center of the fuel cluster makes the coolant void reactivity of the D_2O lattice shift to negative values. As seen in Table III, the calculations are, as a whole, in good agreement with the experiments.

[13]"ENDF/B Summary Documentation," BNL-NCS-17541 (ENDF-201, ENDF/B-III), O. OZER and D. GARBER, Eds., Brookhaven National Laboratory (1973).

III.C. Local Power Distribution

Measured local power distributions are given in Table IV together with the calculations by WIMS-D. The maximum value in the local power distribution is called the local power peaking factor, which is important for the thermohydraulic and fuel design. The experimental error in the results was estimated to be ±3%. The maximum value of the local power peaking factor was obtained in the 54-pin cluster with 12 poisoned fuel pins. The insertion of the gadolinium absorber rod slightly increases the local power peaking factor—at most by ~4%. The calculations of the local power peaking factor agree with the experiment within ~4%.

III.D. Thermal Neutron Flux Distribution

Figure 8 shows the experimental and calculational dysprosium reaction rate distribution in the H_2O- and air-filled 54-pin cluster lattice. The calculational results were obtained by integrating the dysprosium reaction rate over the entire energy range. These distributions are normalized at the outer surface of the pressure tube. Thermal neutron flux depression in the cluster region is larger in the H_2O-filled (0% void) lattices than in the air-filled (100% void) ones. In the D_2O-moderator region, on the contrary, the thermal neutron flux seems to be more flattened in the case of the H_2O-filled lattices. The behavior of the thermal neutron flux in the cluster region results from a shortening of the diffusion length by the presence of the H_2O coolant, and accordingly the thermal neutron diffusion depression effect is enhanced.[7] The behavior of the thermal neutron flux in the D_2O moderator is due to the reflection by the H_2O coolant of thermal neutrons emanating from the D_2O moderator.

Figure 9 shows the influence of the gadolinium

TABLE III

Comparison of Coolant Void Reactivity Reduction Between 54-Pin Cluster and Test Fuel Cluster

Fuel Type	Absorber			Coolant Void Fraction (%)	Change in Reactivity	
	Arrangement in Cluster	Number of Pins	Gd_2O_3 Content (wt%)		Experiment (%)	Calculation (%)
54-pin cluster with poisoned fuel pin	Third layer	1	1.0	0	−18.6	−17.2
	Third layer	1	1.0	100		
	Third layer	12	1.0	0	−85.7	−78.6
	Third layer	12	1.0	100		
54-pin cluster with gadolinium absorber rod	Center of cluster	1	---	0	−10.9	−9.6
				100		

TABLE IV

Local Power Distributions

Fuel Type	Void Fraction (%)	First Layer (F-1)[a]	Second Layer (F-2)			Third Layer (F-3)[b]	
			F-2-1	F-2-2	F-2-3	F-3-1	F-3-2
54-pin cluster	0	Experiment 0.805 ± 0.023	0.785 ± 0.023			1.260 ± 0.025	
		Calculation 0.783	0.804			1.256	
	100	Experiment 0.740 ± 0.022	0.876 ± 0.026			1.223 ± 0.031	
		Calculation 0.768	0.891			1.200	
54-pin cluster with gadolinium absorber rod	0	Experiment 0.715 ± 0.021	0.787 ± 0.024			1.303 ± 0.033	
		Calculation 0.699	0.804			1.297	
	100	Experiment 0.700 ± 0.021	0.862 ± 0.026			1.254 ± 0.032	
		Calculation 0.737	0.889			1.215	
54-pin cluster with poisoned fuel pins	0	Experiment 0.880 ± 0.026	0.938 ± 0.028	0.735 ± 0.022	0.777 ± 0.023	2.042 ± 0.06	0.353 ± 0.011
		Calculation 0.960	0.888	0.812	0.836	1.965	0.307

[a] See Fig. 4 for locations of measurement points.

[b] Experimental values for a 54-pin cluster with or without the gadolinium absorber rod were averaged between two positions, F-3-1 and F-3-2, because they agreed with each other within experimental error.

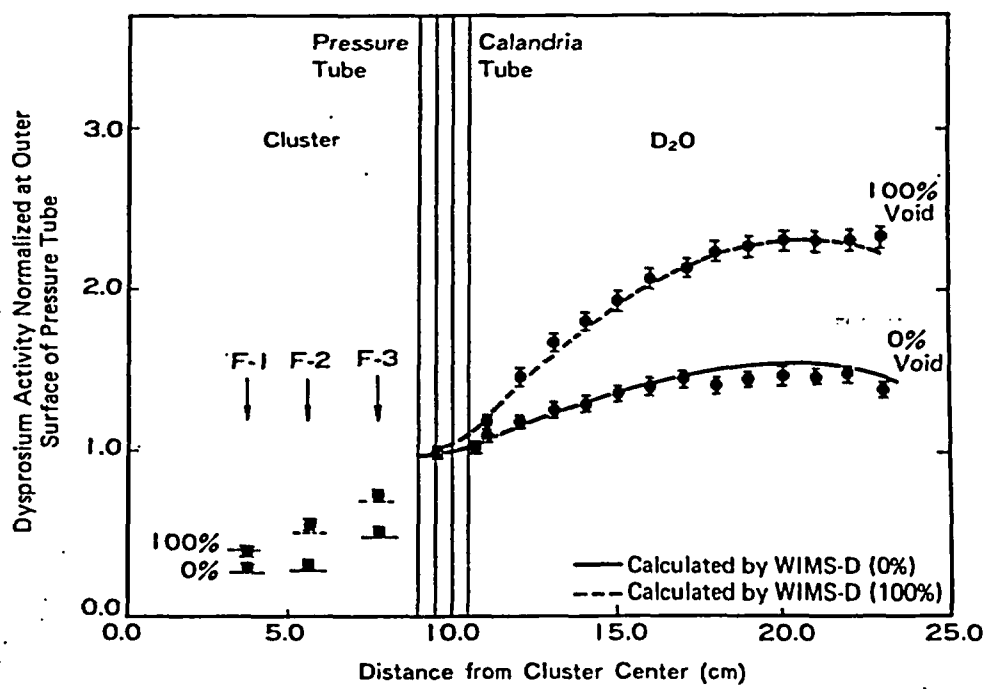

Fig. 8. Dysprosium reaction rate distributions in a 54-pin cluster.

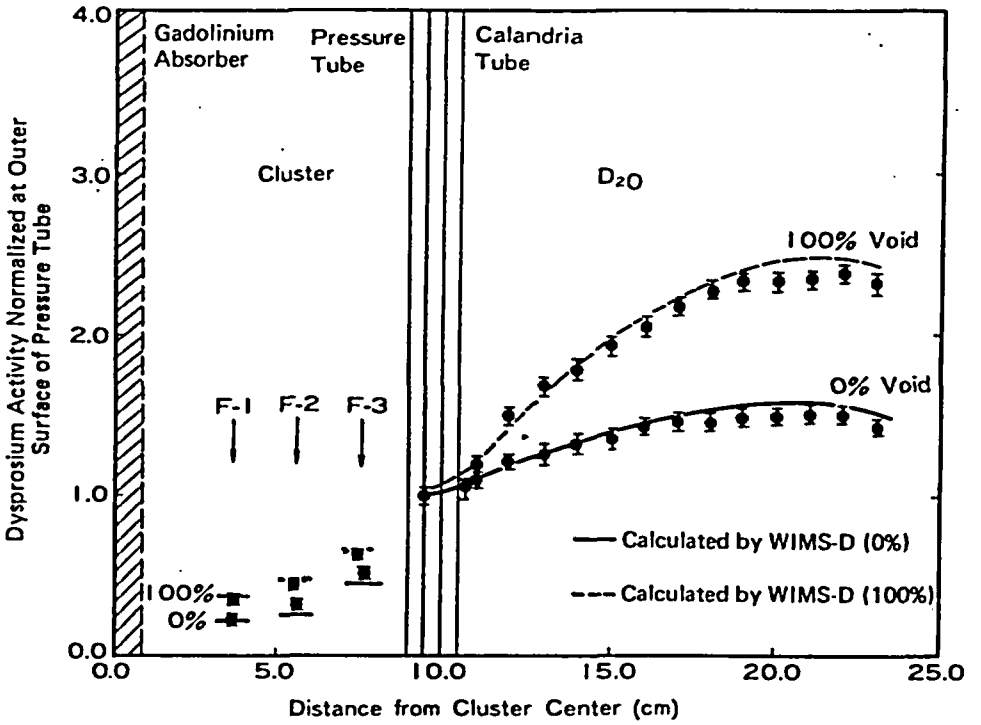

Fig. 9. Dysprosium reaction rate distributions in a 54-pin cluster with a gadolinium absorber rod.

absorber rod on the distribution of the dysprosium reaction rate in the 54-pin cluster lattices. In the air-filled lattice, the distribution decreases more steeply toward the center in the 54-pin cluster with the rod than without it. This behavior shows that neutron absorption by the rod increases in the air-filled cluster due to the smaller depression of the neutron flux there because the self-shielding effect enhanced by the H_2O coolant disappears in this air-filled cluster. This is the reason why the coolant void reactivity is shifted to negative by the insertion of the rod in the center of the fuel cluster.

Figure 10 shows the measured and calculated dysprosium reaction rate distributions of the 54-pin cluster lattice with 12 poisoned fuel pins. The thermal neutron flux within the fuel cluster region is greatly depressed by these pins. These thermal neutron flux distributions were well predicted by WIMS-D.

III.E. Fine Structure of the Thermal Neutron Flux Distribution

The fine structure of the thermal neutron flux distribution in fuel pellets is shown in Fig. 11. These distributions are normalized at the outer surface of the fuel pellet. The thermal neutron flux depression in the fuel pellet is increased with increasing Gd_2O_3 content. The accentuated depression can be ascribed to the greater thermal neutron self-shielding effect due to absorption by the gadolinium in the fuel pellet. But the flux depression effect of

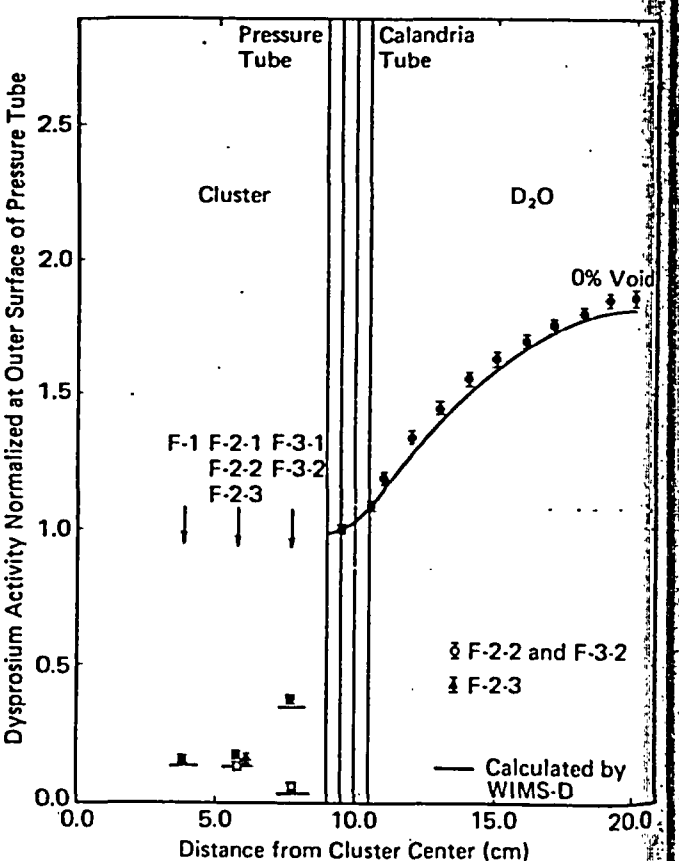

Fig. 10. Dysprosium reaction rate distribution in a 54-pin cluster with poisoned fuel pins.

the poison does not greatly change in the range above 0.5 wt% Gd_2O_3.

The calculation of the fine structure of the thermal neutron flux distribution in the fuel pin strongly depends on the number of mesh intervals in the fuel pellet. Table V shows the comparison of the average experimental and calculated dysprosium reaction rates for 1, 5, 10, and 32 mesh intervals in the fuel pellet. For accurate calculation by WIMS-D, it is necessary to divide the fuel pellet region into more than five mesh intervals due to the enhancement of thermal neutron self-shielding effect due to the absorption of neutrons by gadolinium in the poisoned fuel pins.

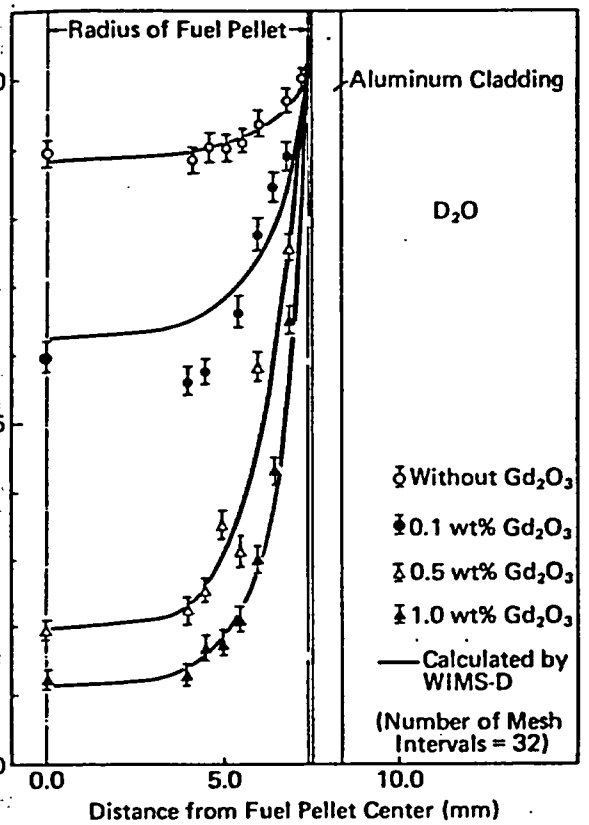

Fig. 11. Fine structure of dysprosium reaction rate distributions in fuel pellets.

IV. CONCLUSION

The physical behavior of burnable poison fuel pins containing Gd_2O_3 in a heavy-water-moderated, cluster-type fuel lattice has been observed from measurements of the reactivity change the coolant void reactivity, the local power distribution, and the thermal neutron flux distribution, including fine structure, using the DCA.

The reactivity effect does not change greatly due to the saturation of thermal neutron self-shielding effect in fuel pins when the Gd_2O_3 content of fuel pellets is more than 0.5 wt%.

A new technique for utilizing a burnable poison in a gadolinium absorber rod inserted into the center of a cluster-type fuel assembly has been developed. The gadolinium absorber rod, although it causes a small increase in local power peaking, is effective for the control of initial excess reactivity and for making the coolant void reactivity negative.

From the comparison of the fine structure of the thermal neutron flux distribution between experiment and calculation, it has been shown

TABLE V

Comparison of Experimental and Calculated Average Dysprosium Reaction Rates

Fuel Type	Experiment[a]	Results Calculated by WIMS-D[a]			
		32 Mesh Intervals	10 Mesh Intervals	5 Mesh Intervals	1 Mesh Interval
1.5 wt% ^{235}U UO_2 fuel pin	0.922 ± 0.032	0.918	0.923	0.927	0.928
0.1 wt% Gd_2O_3 poisoned fuel pin	0.723 ± 0.029	0.747	0.762	0.776	0.781
0.5 wt% Gd_2O_3 poisoned fuel pin	0.424 ± 0.016	0.442	0.439	0.464	0.466
1.0 wt% Gd_2O_3 poisoned fuel pin	0.317 ± 0.011	0.308	0.302	0.245	0.146

[a]The values are normalized at the reaction rate of the outer surface of fuel pellet.

that for accurate calculation using the WIMS-D code it is necessary to divide the fuel pellet region into more than five mesh intervals because the thermal neutron self-shielding effect is increased by the absorption of gadolinium in poisoned fuel pins. The calculations by the WIMS-D and CITATION codes are in good agreement with the experimental results and are within 9% of the measured reactivities.

ACKNOWLEDGMENTS

The authors are much indebted to Y. Hachiya for h
fruitful discussion. We wish to thank N. Fukumura, K. Shib
A. Nishi, and the staff of the Heavy Water Critical Experime
Section, Oarai, Power Reactor and Nuclear Fuel Developme
Corporation for their support in this series of experiment
The kind support of S. Sawai and Y. Miyawaki is deep
appreciated.